

HYDRAULIC CHARACTERISTICS OF THE AIRLIFT PUMP

Sebastian Kujawiak, Małgorzata Makowska✉, Radosław Matz

Department of Hydraulic and Sanitary Engineering, Poznan University of Life Sciences, ul. Piatkowska 94A, 60-649 Poznań

ABSTRACT

Airlift pumps are the simplest devices used for lifting and transporting of liquid in water and wastewater systems. They constitute the subject of interest in numerous studies, focusing on their two-phase flow. The knowledge of two-phase flow parameters is necessary for the correct design of an airlift pump. In the available literature on the subject, one will find numerous models describing the two-phase gas-liquid flow. One of the most popular is the Zuber – Findlay model, also called the slip model.

The subject of the present research consisted in a vertical bubble column, with the diameters of 50 and 75 mm, used to transport the water-air mixture. Based on the results of the laboratory experiments the hydraulic characteristics were developed: liquid flow depending on the depth H_s and the air flow Q_p . For the mathematical description, second-degree polynomial model was applied, as well as an assessment of the determination coefficient was performed. Efficiency factors of the airlift pump and other parameters for two-phase mixture during the airlift pump's operation were determined using the slip model. Based on the experiment, it has been found for both of the analysed diameters that the efficiency of the airlift pump increased along with the depth H_s and the air flow Q_p . The airlift pump achieves maximum liquid efficiency within a specified range of the immersion depth. In a small diameter airlift pump (50 mm), slug and plug flow regimes are predominant.

Keywords: airlift pumps, two-phase flow, airlift pumps efficiency

INTRODUCTION

Airlift pumps are the simplest devices, in terms of structure, that perform similar functions to classic pumps. They can lift and transport liquid over short distances. Literature is rich in examples of the use of airlift pumps in various branches of industry and biotechnology (Grzywacz, 2012). In water and wastewater technology, lifts are used for transport in water and sewage systems. In Poland, they are used for the transport of sewage and sludge in sewage treatment plants as well as for transporting the bed in self-regulating filters and for the renovation of drilled wells (Heidrich et al., 2008; Kalenik, 2015; Merchuk and Gluz, 2002; Solecki, 2010). Airlift pumps are perfectly suitable for water conditioning for aquaculture and reclamation of reservoirs and lakes (Fan et al., 2013; Parker, 1983).

Due to their construction, they ideally mix and aerate water, removing carbon dioxide therefrom in industrial fish farming (Barrut et al., 2012). Numerous advantages, including simple structure and lack of mechanical elements make them highly reliable. In chemical engineering, they are used to transport corrosive and radioactive liquids, and in the petrochemical industry, they are used for transporting fuels (Cachard and Delhaye, 1996; Hanafizadeh et al., 2011; Kassab et al., 2007; Khalil et al., 1999).

An important area in which airlift pumps are applied is the transport of solids, including sand. Kalenik (2017) built a research unit for transporting a mixture of sand and water, and he provided formulas for calculating the size of the stream of transported media. Sawicki (2004) analysed this issue with regard to the design of aerated sand traps.

✉ e-mail: mmak@up.poznan.pl

Results of research into the efficiency of airlift pumps have been described in numerous publications (Bar-Meir, 2013; Fan et al., 2013; Hanafizadeh et al., 2011; Kalenik and Przybylski, 2011; Kassab et al., 2007; Lewandowski, 1965). The performance of an airlift pump depends on many factors, whereas the most important are: the diameter of the pump, the type of the water and air mixer, the geometric height of the lift, and the immersion depth of the airlift pump, as well as the method of injection and the incoming air flow rate. The structure and the flow parameters also depend on the design and the method of air supply to the airlift pump. Kalenik and Przybylski (2011) conducted tests of three different types of mixers. The three tested structures differed in the number, position, and diameter of openings. The mixer with the structure of a single air supply nozzle generated air flow in the form of large irregular bubbles that moved in a chaotic and turbulent manner. The stream of water outflowing from the pump was not continuous but pulsating, with the slug flow structure. The height of the water lift in this structure was the largest, growing along with increasing of the air flow rate, in proportion to the flow velocity of the mixture. The remaining two mixer structures, equipped with more small holes, arranged in two different ways, generated a fine bubble structure. The flow velocity of the mixture was much lower, thus the expenditure and lift height were reduced. Budzyński (2011) carried out research on the pulse-bubble column. The pulsations caused a reduction and unification of the size of the gas bubbles, thus increasing the area of interphasic contact, and increasing the time duration of the gas bubbles remaining in the reaction volume. The result of the research was a generalization of the formula, enabling the calculation of basic quantities necessary to design a pulsed-bubble column. He has taken into the influence of pulsation parameters, physicochemical properties of the system, and bubble column geometry – that is, the most important elements determining the course of hydrodynamic phenomena in the pulse-bubble column – on the size of the gas bubbles formed, and the proportion of phases in the mixture. As demonstrated by the research conducted by Ahmed and others (2016), the design of the device, and the method of air injection as well as the dosing system thereof have a significant impact on the efficiency of

the airlift pump. Airlift pump performance was tested for various injection methods: radial, axial, double and vortex, in a fixed system, and in a pulsed injection mode. In the fixed system, the highest efficiency was obtained with the double injection method. In the pulse-bubble system, the maximum lifting capacity was obtained for low air velocities. Research has shown that the vortex structure works very much like radial or axial design in terms of energy expenditure and power consumption. Changing the angle of air supply did not cause any changes in the device's operation. Reinemann et al. (1990) conducted hydraulic tests of small airlift pumps with diameters of 3 to 20 mm. They analysed the influence of the pipe diameter on the vertical slug flow. Their considerations were based on the theories previously put forward by Nicklin (1963), expanding them in terms of pipe diameters and the influence of surface tension. They have noticed marked differences between experimental observations and theoretical considerations. The authors proposed their own model, describing the flow in small-diameter airlift pumps. Cacharda and Delhaye (1996) also conducted hydraulic tests on small pumps with diameters not exceeding 40 mm, used to transport corrosive liquids. Based on the obtained results, the authors demonstrated that the current models are not suitable for the design of small diameter lifts, because they overstate pressure losses in the slug flow. The proposed new model creates a tool for the analysis and design of lifts with diameters up to 40 mm. Tighzert et al. (2013) conducted tests of an airlift pump of 33 mm diameter and 3.1 m length, together with a quick-closing valve installed to measure the volume fraction of gas. The tests have shown an increase in the airlift pump's efficiency along with the increase of the supplied air flow rate, until reaching the maximum. After exceeding the maximum values, the slug flow structure passed into the churn flow, thus the slip ratio increased. The performance increased with the increase of the immersion ratio, expressed as the ratio of the immersion depth to the height of the pressing conduit of the pump. The optimal range of the coefficient was 0.4–0.75. For a constant air flow rate supplied, the gas volume share ratio decreased with the increase of the immersion ratio. The tests confirmed the correctness of using a slip model for this type of considerations.

PARAMETERS OF TWO-PHASE FLOW

Knowledge of the basic parameters describing two-phase flow in airlift pumps is essential for their correct design. The flow of a liquid-gas mixture is characterized by (Dziubiński and Prywer, 2009):

- volume and mass fraction of each phase,
- structure (bubble, piston, projective, foam, annular, droplet),
- mass flow rate and volume flow rate,
- mass velocity.

Due to differences in volumes and viscosities of both phases, the gas phase flows at a much higher velocity than the liquid phase, which results in the formation of a phase slip mechanism, characterized by the slip velocity of v_p . The latter, like the SLP slip ratio, is a measure of the proportion of phases in the flowing mixture:

$$v_p = v_G - v_L = \frac{u_G}{\alpha_G} - \frac{u_L}{\alpha_L} \quad (1)$$

$$SLP = \frac{v_G}{v_L} = \frac{u_G}{u_L} \cdot \frac{\alpha_L}{\alpha_G} \quad (2)$$

where:

- v_p – gas slip velocity, in $\text{m} \cdot \text{s}^{-1}$,
- v_G – gas flow velocity, in $\text{m} \cdot \text{s}^{-1}$,
- v_L – liquid flow velocity, in $\text{m} \cdot \text{s}^{-1}$,
- u_G – superficial average gas velocity, in $\text{m} \cdot \text{s}^{-1}$,
- u_L – superficial liquid velocity, in $\text{m} \cdot \text{s}^{-1}$,
- α_G – liquid void fraction,
- α_L – liquid void fraction.

Determining the volume fraction of a given phase is possible by direct flow measurement, or by using different types of models describing two-phase flow.

MODELS DESCRIBING TWO-PHASE FLOW

Many models describe a two-phase liquid-gas flow. They include simple one-dimensional models, as well as advanced and complex multidimensional and multifaceted models (Dziubiński and Prywer, 2009).

The homogeneous model of the flow of a two-phase liquid-gas mixture assumes that both phases move at the same velocity and are evenly mixed. This

allows us to assume that the mixture has a pseudo-single-phase composition, with averaged properties.

The phase separation model assumes that each phase has a different flow rate and different properties, while it also assumes a homogeneous pressure of both phases at any point of the conduit through which the mixture is flowing. The model describes the movement of each phase separately, and it takes into account the interaction occurring between the phases.

In the models with partial phase separation, the equations of flow continuity, motion and energy are recorded as for non-slip models. In addition, differences are assumed between parameters describing biphasic flow, for instance, the velocity of each of the two phases.

Models with complete phase separation find a wider application compared to homogeneous models when modelling two-phase flows. In these models, the flow of a two-phase mixture is described independently for each phase using continuity (conservation) equations.

The Zuber-Findlay slip model is an extension of the Wallis (1969) model. This model is based not on the flow velocity of individual liquid-gas phases, but on the velocity of one phase flow relative to the other, referred to as relative velocity (drift). The averaged real velocity of one of the phases in relation to the superficial speed of the mixture is called drift speed. The Zuber-Findlay model, unlike the homogeneous model and the two-phase flow model with phase separation, is called the slip model or drift model (Zuber and Findlay 1965). The general formula of the model takes the following form:

$$\frac{u_G}{\alpha_G} = C_0 \cdot u_{TP} + v_{dr} \quad (3)$$

where:

- C_0 – distribution coefficient,
- u_{TP} – superficial speed of the mixture, in $\text{m} \cdot \text{s}^{-1}$,
- v_{dr} – drift speed, in $\text{m} \cdot \text{s}^{-1}$.

The Zuber-Findlay model enables the determination of the gas phase ratio α_G in the flow of a two-phase mixture with an accuracy of up to approximately 20%. For greater consistency of the model, the values of coefficient C_0 and correlation equations for drift speed v_{dr} were developed based on numerous studies. The

slip model is a compromise between the homogeneous model, which is very simple but also has limited applicability, and a more complex model with phase separation. In subject literature, it is considered the most universal (Dziubiński and Prywer, 2009; Fidos, 2001; Govier and Aziz, 1972; Hibiki and Ishii, 2002; Kawanishi et al., 1990).

Hibiki and Ishii (2002, 2003) developed a set of three-dimensional constitutive equations describing the slip model in the form of a simplified one-dimensional Zubert-Findlay model. They proposed equations describing C_o distribution coefficient.

EFFICIENCY OF AIRLIFT PUMPS

Efficiency of airlift pumps η , similarly to classic pumping systems, is determined by the ratio of hydraulic power to electric power (Skowroński, 2009).

$$\eta = \frac{P_h}{P_w} \quad (4)$$

where:

P_h – hydraulic power contained in the mass of water, in W;

P_w – electric power on the pump shaft, in W.

Theoretical efficiency of airlift pumps, assuming the isothermal air expansion in accordance with Boyle-Mariotte's law (Coulson and Richardson, 1999; Lewandowski, 1965; Nicklin, 1963; Reineemann et al., 1990), is calculated using the following formula:

$$\eta = \frac{N_2}{N_1} \quad (5)$$

where:

N_2 – power contained in the mass of water lifted per unit of time to the height of H_p in W,

N_1 – power needed to compress air from pressure p_b to pressure p_0 , in W,

$$N_2 = \gamma_w \cdot Q_w \cdot H_t \quad (6)$$

$$N_1 = p_b \cdot Q_p \cdot \ln \left(\frac{p_0}{p_b} \right) \quad (7)$$

where:

H_t – the height of water rise, in m,

γ_w – the volumetric weight of water-air mixture, in $\text{kg} \cdot \text{m}^3$,

p_b – barometric pressure, in Pa,

Q_p – volumetric air flow rate at barometric pressure, in $\text{m}^3 \cdot \text{h}^{-1}$,

Q_w – volumetric flow rate of water, in $\text{m}^3 \cdot \text{h}^{-1}$,

p_0 – pressure at the depth of the diffuser, in Pa.

The efficiency of airlift pumps depends on many factors. For identical air flows, increasing the immersion depth of the airlift pump increases the efficiency of the lift. The efficiency of airlift pumps is also dependent on the structure of the two-phase flow in the lift. For slug flow and slug-foam flow, the efficiency reaches its maximum value. The maximum efficiency does not occur for the maximum mass flow of water in the lift. Increasing the lift height H_t reduces the efficiency of the airlift pumps in the same flow conditions (Sadek et al., 2009).

MATERIAL AND METHODS

The subject of the research was an airlift pump used for transporting water – air mixture. The research model (see: Fig. 1) consisted of a cylindrical tank (9) with a diameter of 100 cm and a height of 150 cm. In the axis of the tank, a hydraulic airlift pump (10) was installed, with a diameter D_p , of 50 and 75 mm respectively (the flow in the horizontal and sloping part of the discharge pipe was unpressurized). The system was powered via a membrane air blower (1). For smooth regulation of the supplied air flow rate, two valves have been mounted to the airlift pump: control valve (2) and bleed valve (3). A rotameter (4) was used to measure the air flow supplied to the pump. The water level in the tank (9) was determined by means of a scale (5) mounted on the wall inside the tank (9). In the auxiliary tank (8) a rotodynamic pump (7) was installed in order to refill the main tank (9) with water. The internal structure of the water and air mixer, by Akwatech company, consisted of a simple check valve, along with a perforated rubber membrane with 8 pores, each 1 mm in diameter. The mixer was placed 22 cm from the bottom of the tank.

Before testing the airlift pump, the air flows Q_p supplied to the mixer (6) had been determined. After the

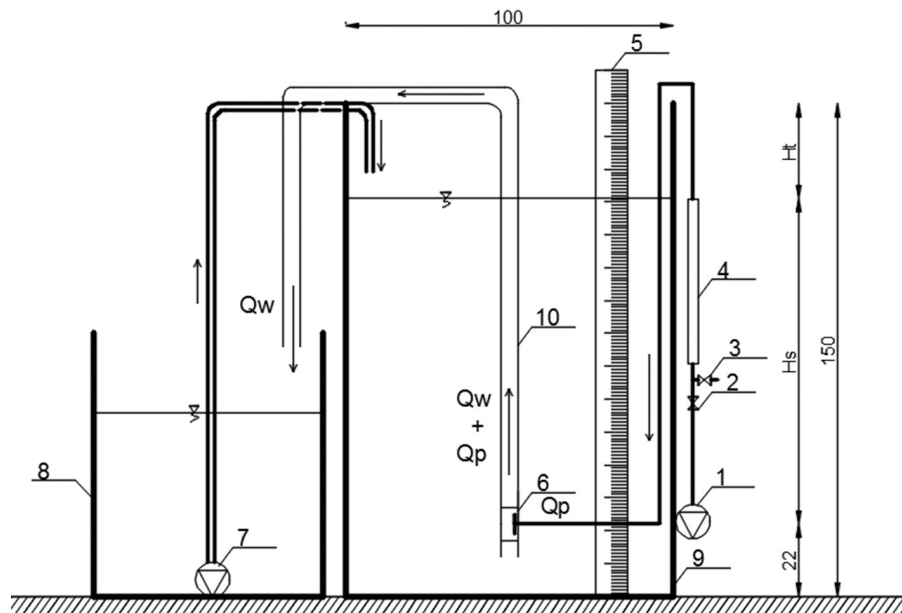


Fig. 1. Scheme of the air lift pump testing unit: 1 – air blower, 2 – control valve, 3 – blow off valve, 4 – rotameter, 5 – scale, 6 – diffuser, 7 – rotodynamic pump, 8 – recirculation tank, 9 – main tank, 10 – delivery pipe, H_t – water – air mix delivery head, H_s – immersion depth of the water – air diffuser

air (1) was started, the air flow rate on the rotameter (4) was set using the bleed valve (3) for the given immersion depth H_s of the mixer. Due to changes in the air flow rate when changing the H_s immersion depth of the mixer, air flows Q_p were recorded for all the measuring series tested, and averaged using the arithmetic mean, thus obtaining the following values: 4.6; 4.15; 3.65; 3.15; 2.65; 2.15; 1.65; 1.4; 0.75 $\text{m}^3 \cdot \text{h}^{-1}$.

By means of the scale (5), changes in the water table in the tank were read with an accuracy of 0.5 cm. Five measurement series were conducted, for different immersion depths of H_s : 123; 113; 103; 93; 83; 73; 63 and 56 cm. The measurement was started after filling the tank with water to the required immersion depth of H_s and after setting the required air flow of Q_p . The amount of outflowing water Q_w was measured and recorded, with the water level in the tank changing over time, at a depth of 10 cm. For the averaging of results, the Q_w expenditure was assigned to the geometrical centre of the layer being tested. Having completed the measurement, the water from the tank (8) was pumped using a centrifugal pump (7) to the main tank (9). Measurements for each position of the water-air mixer were conducted in five repetitions, with 9 different air flows.

The simple measurement system made it possible to obtain the results on the basis of which the hydraulic characteristics were developed for the airlift pump system with diameters of 50 and 75 mm:

- A) airlift pump capacity depending on the immersion depth of H_s . (for H_s from 56 to 123 cm),
- B) airlift pump capacity depending on the amount of air supplied Q_p (for Q_p from 0.75 to 4.6 $\text{m}^3 \cdot \text{h}^{-1}$).

The mathematical model in the form of a second-degree polynomial was used to describe the hydraulic characteristics *A* and *B* of the airlift pump, and the determination coefficient was evaluated. The obtained results significantly extended the mixer characteristics given by the manufacturer, and enabled the analysis of the device's operation in a wide range of parameters.

RESULTS AND DISCUSSION

Figures 2 and 3 show the relationship $Q_w = f(H_s)$ for both D_p diameters used in the airlift pump. Characteristic curves of the upward trend in the tested range of the independent variable H_s were obtained. The determination coefficient between 0.98–0.99 indicates that

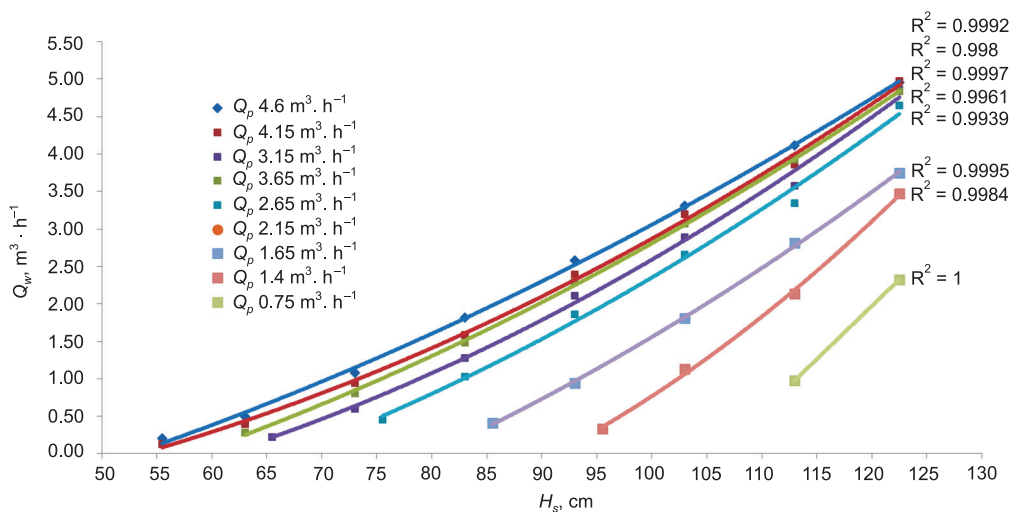


Fig 2. The rate of water flow of the airlift pump depending on immersion depth $H_s \cdot D_p=50$ mm

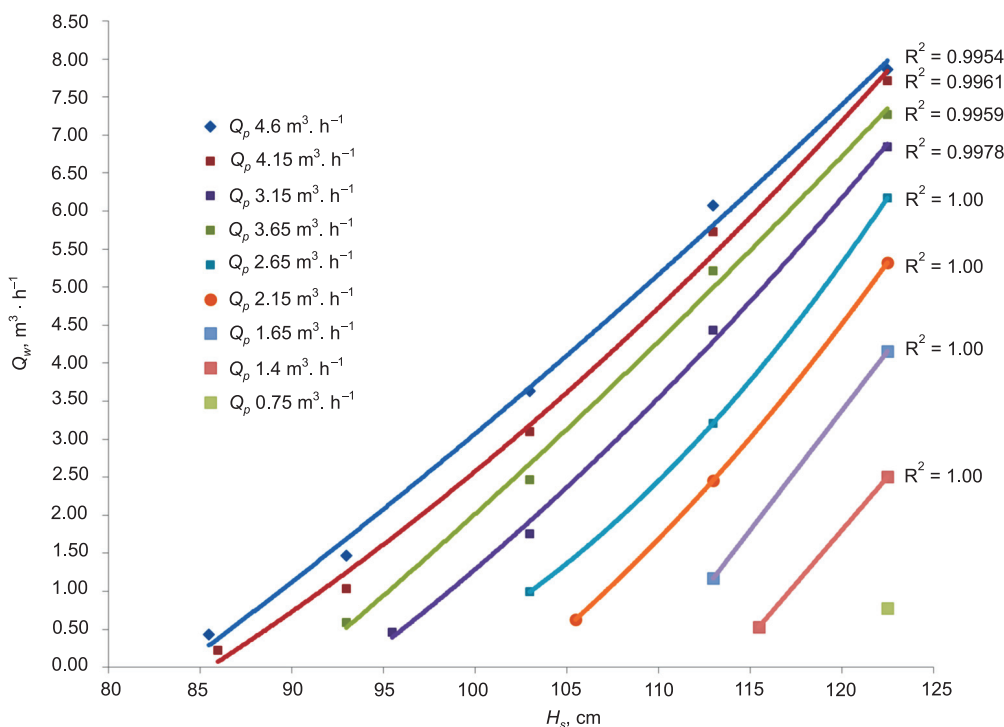


Fig. 3. The rate of the water flow of the airlift pump depending on immersion depth $H_s; D_p=75$ mm

the airlift pump's efficiency within the measured range depends significantly on the immersion depth of the water-air mixer. In the tested H_s range, the maximum lifting capacity of $5.0 \text{ m}^3 \cdot \text{h}^{-1}$ for a diameter of 50 mm, and $7.8 \text{ m}^3 \cdot \text{h}^{-1}$ for a diameter of 75 mm was obtained.

Figures 4 and 5 show the relationship $Q_w = f(Q_p)$ for both D_p diameters used in testing the airlift pump. The obtained coefficients of determination (0.77 to 0.99) indicate a significant dependence of the airlift pump's capacity in the measuring range on the amount

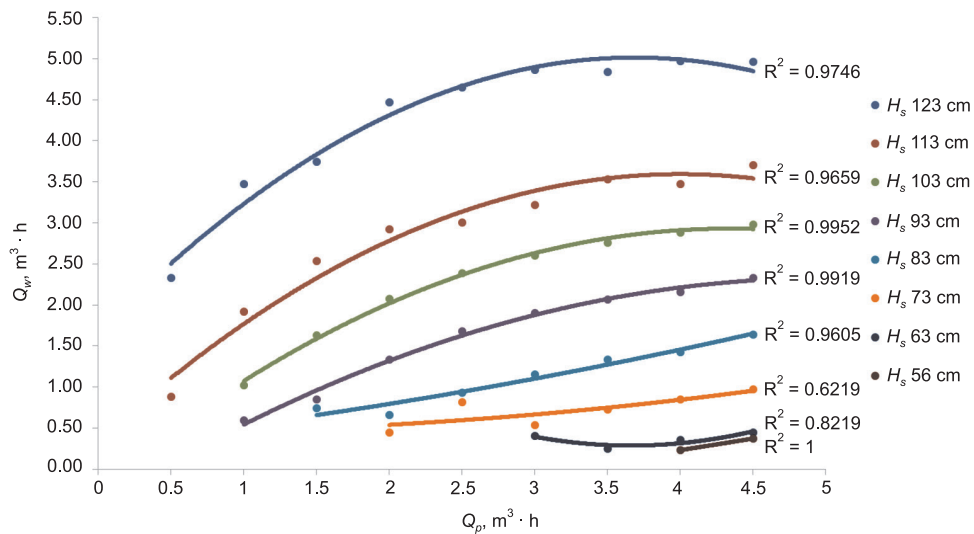


Fig 4. The rate of the water flow of the airlift pump, depending on air-flow supplied Q_p ; $D_p = 50$ mm

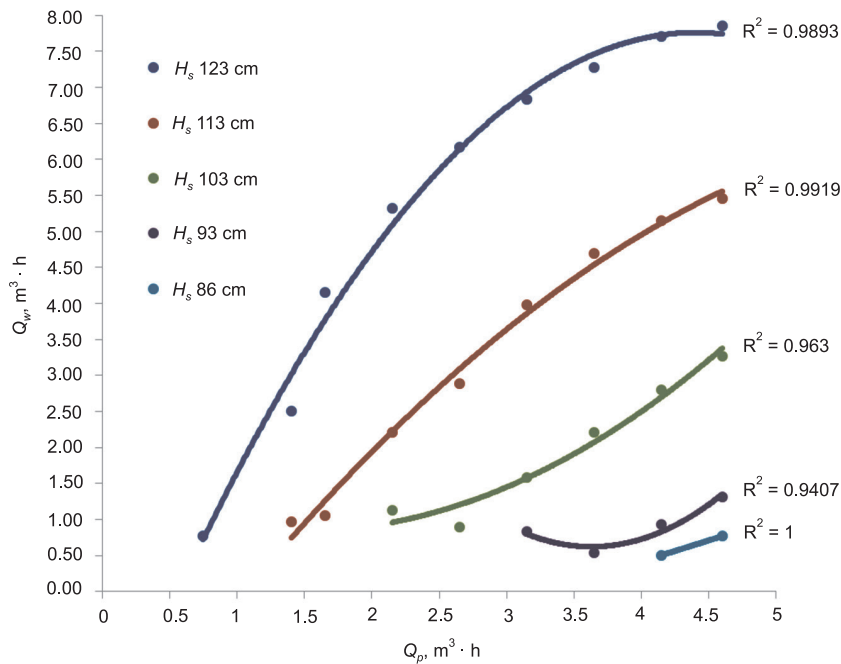


Fig 5. The rate of the water flow of the airlift pump, depending on air-flow supplied Q_p ; $D_p = 75$ mm

of air dispensed. The airlift pump's flow rate of the water in the Q_p test range increased to its maximum value, after which it gradually decreased. For example, at the maximum assumed immersion depth of the water-air mixer (that is 123 cm), and the amount of supplied air of $4.5 \text{ m}^3 \cdot \text{h}^{-1}$, the maximum lifting capacity of

$5.0 \text{ m}^3 \cdot \text{h}^{-1}$ was obtained for the diameter $D_p = 50$ mm, and $8 \text{ m}^3 \cdot \text{h}^{-1}$ for the diameter $D_p = 75$ mm. For the remaining depths of H_s , these values are correspondingly smaller. Above these values, the curve breaks, and the airlift pump's flow rate decreases. This phenomenon can be explained by a significant increase in slip ve-

locity, and the change in the vertical flow structure of the airlift pump (Tighzert et al., 2013). This also means that for the tested lifts, the air flow rate supplied should not exceed certain values, as confirmed by Kalenik and Przybylski (2011) and by Tighzert et al. (2013).

Comparing the characteristics of airlift pumps with a diameter of 50 and 75 mm, it results that for the mixer immersion depth $H_s > 100$ cm, the flow rate of the airlift pump with a diameter of 75 mm is nearly 50% greater, compared to the airlift pump with a diameter of 50 mm. For the sinking depth of $H_s < 100$ cm, the flow rate of the water of the airlift pump with 50-mm diameter increased in relation to the capacity of the airlift pump with 75-mm diameter. The difference in performance characteristics results from significant differences in the cross-sectional area of both airlift pumps (respectively 19.64 and 44.18 cm²). Decreasing the depth of H_s reduces the range of air flow values for which the lift transports the liquid; the smaller the liquid pressure in the tank, the more air is needed to achieve the water flow.

The pulsating nature of the water flow through the delivery pipeline was a disturbing factor, causing error in the readings and differences in the performance, especially in the case of the 75-mm lift diameter, which was also found by Kalenik and Przybylski (2011). For

this reason, the curves obtained for the smallest H_s values deviate from the others, and are characterized by the lowest coefficient of determination. Since greater accuracy was obtained for diameter of $D_p = 50$ mm, further analyses were carried out for this specific variant. Equations used to describe the phenomenon are intended for the so-called small diameters (up to 63 mm), therefore this decision was considered all the more appropriate.

On the basis of equation 5, the efficiency of the airlift pump was calculated depending on the immersion depth, for the previously assumed range of air flow (see: Fig. 6). Note that the efficiency of the airlift pump increases with the immersion depth to the maximum value, which does not correspond to the maximum immersion depth H_s , and the maximum Q_w expenditure. It turned out that the maximum efficiency of the airlift pump was obtained at H_s of about 85 cm, for the largest Q_p values of the tested range, and for H_s of about 110 cm for the lowest value of Q_p respectively.

Using the aforementioned Zuber-Findlay slip model (equation 3) and the equations used to calculate the model's parameters (Hibiki and Ishii 2002, 2003), apparent velocities, real velocities, and share ratios for the fractions of liquids and gas in a 50 mm diameter air lift were determined for a constant $Q_p = 4.6 \text{ m}^3 \cdot \text{h}^{-1}$, and for different values of H_s (see: Table 1). Based on the

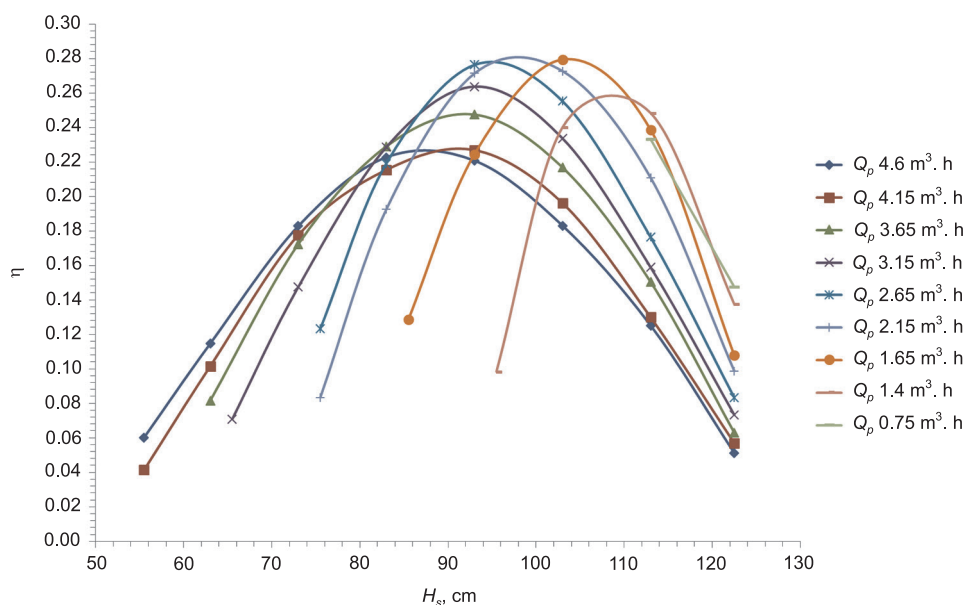


Fig. 6. The efficiency of the airlift pump with 50 mm diameter depending on immersion depth H_s and air flow Q_p

Table 1. Calculated parameters for airlift pumps: $D_p = 50$ mm, $Q_p = 4,6$ m³ · h⁻¹; S – slug flow of biphasic mixture flow, SPL – drift slip ratio

No.	H_s	H_t	Flow structure	α_G	α_L	u_G	u_L	v_G	v_L	v_p	SPL
–	cm	cm	–	–	–	m · s ⁻¹	–				
1	123	6	S	0.23	0.77	0.65	0.70	2.84	0.91	1.93	3.12
2	113	15	S	0.24	0.76	0.65	0.58	2.72	0.77	1.95	3.55
3	103	25	S	0.25	0.75	0.65	0.47	2.60	0.62	1.98	4.17
4	93	35	S	0.26	0.74	0.65	0.37	2.50	0.49	2.01	5.06
5	83	45	S	0.27	0.73	0.65	0.26	2.39	0.35	2.04	6.78
6	73	55	S	0.28	0.72	0.65	0.15	2.29	0.21	2.08	10.73
7	63	65	S	0.30	0.70	0.65	0.07	2.21	0.10	2.11	22.16
8	56	73	S	0.30	0.70	0.65	0.03	2.16	0.04	2.12	51.84

universal map for upward flow, developed by Ulbrich (1989), it was found that the flow structure for the tested work system of the airlift pump is projective, and the share of the gas phase is 23–30%. As the Q_w airlift expenditure increases, also the liquid speed increases. Actual velocity of gas in relation to its apparent velocity differs significantly. The speed of interphasic slip depends mainly on the speed of the liquid, and it increases with the decrease thereof (see: Table 1).

CONCLUSIONS

The subject of the research concerned the two-phase water-air flows in a hydraulic airlift pump with a diameter of 50 and 75 mm. The impact of changes in the immersion depth H_s and the intensity of the supplied air Q_p on the performance of the airlift pump Q_w have been investigated. Based on the conducted tests, it was determined that:

- the efficiency of the airlift pump with a diameter of 50 and 75 mm increases with increasing the immersion depth H_s (see: Fig. 2 and 3); during the operation of the 75-mm diameter airlift pump, a noticeable pulsatory flow mode was noticed, hence a 50-mm diameter airlift pump proved more effective;
- the Q_w airlift pump efficiency increases with the increase of the air supply of Q_p (see: Fig. 4 and 5); the expenditure after reaching a certain maximum decreases as a result of changes in the proportions of the components of the biphasic mixture and the flow structure;

- the airlift pump reaches its maximum efficiency within the specified range of the H_s immersion depth of the water-air mixer; maximum airlift pump efficiency does not correspond to the maximum immersion depth H_s and the air flow rate Q_p ; these correlations are consistent with the results of previous studies (Sadek et al., 2009);
- in a small diameter (50 mm) airlift pump, a projective flow structure dominates, which is the most desirable from the point of view of Q_w capacity and efficiency of the lift.

REFERENCES

- Ahmed, W.H., Aman, A.M., Badr, H.M., Al-Qutub, A.M. (2016). Air injection methods. The key to a better performance of airlift pumps. Original Research Article Experimental Thermal and Fluid Science, 70(1), 354–365.
- Bar-Meir, G. (2013). Basics of Fluid Mechanics. Chapter 14. Multiphase. Downloads ver. 0.3.4.2 January 9.
- Barrut, B., Blancheton, J.-P., Champagne, J.-Y., Grasmick, A. (2012). Mass transfer efficiency of a vacuum air lift – application to water recycling in aquaculture systems. Aquacultural Engineering 46, 18–26.
- Budzyński, P. (2011). Hydrodynamika przepływu pęcherzy gazowych w barbotażowej kolumnie pulsacyjnej. Zeszyty Naukowe. Rozprawy Naukowe Politechnika Łódzka, 416.
- Cachard, J.M., Delhay, F. (1996). A slug-churn flow model for small-diameter airlift pumps. International Journal Multiphase Flow, 22(4), 627–649.

- Coulson, J.M., Richardson, J.F. (1999). *Fluid Flow, Heat Transfer & Mass Transfer*. Covers these three main transport processes. Chemical Engineering, 1.
- Dziubiński, M., Prywer, J. (2009). *Mechanika płynów dwufazowych*. Warszawa: Wydawnictwo Naukowo-Techniczne.
- Fan, W., Chen, J., Pan, Y., Huang, H., Chen, C.-T.A., Chen Y. (2013). Experimental study on the performance of airlift pump for artificial upwelling. *Ocean Engineering* 59(7), 47–57.
- Fidos, H. (2001). *Hydrodynamika przepływu mieszanin wielofazowych ciecz nienewtonowska-gaz cząstki ciała stałego w przewodach pionowych*. Praca doktorska. Politechnika Łódzka.
- Govier, G.W., Aziz, K. (1972). *The flow of complex mixtures in pipes*. New York : Van Nostrand Reinhold Co.
- Grzywacz, R. (2012). Właściwości stacjonarne bioreaktorów barbotażowych typu airlift. *Seria Inżynieria i Technologia Chemiczna, Politechnika Krakowska*, 410, 7–22.
- Hanafizadeh, P., Ghanbarzadeh, S., Saidi, M.H. (2011). Visual technique for detection of gas–liquid two-phase flow regime in the airlift pump. *J. Pet. Sci. Eng.*, 75, 327–335.
- Heidrich, Z., Kalenik, M., Podedworna, J., Stańko, G. (2008). *Sanitacja wsi*. Warszawa : Wydawnictwo Seidel-Przywecki.
- Hibiki, T., Ishii, M. (2002). Distribution parameter and drift velocity of drift – flux model in bubbly flow. *Int. J. Heat Mass Transfer*, 45, 707–721.
- Hibiki, T., Ishii, M. (2003). One – dimensional drift – flux model for two – phase flow in a large diameter pipe. *Int. J. Heat Mass Transfer*, 46, 1773–1790.
- Kalenik, M., Przybylski P. (2011). Eksperymentalne badania hydraulicznych warunków pracy powietrznego podnośnika. *GWITS* 6, 219–223.
- Kalenik, M. (2015). Badania modelowe sprawności powietrznego podnośnika cieczy. *Ochrona Środowiska*, 37(4), 39–46.
- Kalenik, M. (2017). Badania modelowe strumienia objętości piasku i wody w podnośniku powietrznym. *Ochrona Środowiska*, 39(1), 45–52.
- Kassab, S.Z., Kandil, H.A., Warda, H.A., Ahmedb, W.H. (2007). Experimental and analytical investigations of airlift pumps operating in three-phase flow. *Chemical Engineering Journal*, 131, 273–281.
- Kawanishi, K., Hirao, T., Tsunge, A. (1990). An experimental study on drift flux parameters for two-phase flow in vertical round tubes. *Nuclear Enng. Des.*, 120, 447.
- Khalil, M.F., Elshorbagy, K.A., Kassab, S.Z., Fahmy, R.I. (1999). Effect of air injection method on the performance of an air lift pump. *International Journal of Heat and Fluid Flow*, 20, 598–604.
- Lewandowski, B. (1965). Charakterystyka hydrauliczna urządzenia o przepływie wymuszonym przez sprężone powietrze. *Arch. Hydrotech.* 12(4), 227–275.
- Merchuk, J.C., Gluz, M. (2002). *Bioreactors, Airlift Reactors*. Encyclopedia of Bioprocess Technology. Beer-Sheva, Israel : Ben-Gurion University of the Negev.
- Nicklin, D.J. (1963). The airlift pump theory and optimization. *Int. Chem. Eng.* 41, 29–39.
- Parker, N.C. (1983). Airlift pumps and other aeration techniques. In. C. S. TUCKER (Ed.). *Water quality in channel catfish ponds*, Southern Cooperative Series Bulletin 290, Mississippi Agriculture and Forestry Experiment Station, Mississippi State University, Mississippi, 24–27.
- Reinemann, D.J., Parlange, J.Y., Timmons M.B. (1990). Theory of small-diameter airlift pumps *International Journal of Multiphase Flow*, 16(1), 113–122.
- Sadek, Z.K., Hamdy, A.K., Hassan, A.W., Wael, H.A. (2009). Airlift pumps characteristics under two-phase flow conditions. *International Journal of Heat and Fluid Flow* 30, 88–98.
- Sawicki, J.M. (2004). Aerated grit chambers hydraulic design equations. *Journal of Environmental Engineering*, 130(9), 1050–1058.
- Skowroński, M. (2009). *Układy pompowe*. Wrocław: Oficyna Wydawnicza Politechniki Wrocławskiej.
- Solecki, T. (2010). Analiza i ocena możliwości renowacji odwiertu w uzdrowisku Połczyn. *Wiertnictwo Nafta Gaz* 27 (3), 617–627.
- Tighzert, H., Brahimi, M., Kechroud, N., Benabbas, F. (2013). Effect of submergence ratio on the liquid phase velocity, efficiency and void fraction in an airlift pump. *Journal of Petroleum Science and Engineering* 110, 155–161.
- Ulbrich, R. (1989). Identyfikacja przepływu dwufazowego gaz – ciecz. *Studia i monografie*, 32. Opole : Wyższa Szkoła Inżynierska.
- Wallis, G.B. (1969). *One-dimensional Two-phase Flow*. New York : McGraw Hill.
- Zuber, N., Findlay, J.A. (1965). Average volumetric concentration in two – phase flow systems. *J. Heat Transfer, Trans. ASME*, 87.

CHARAKTERYSTYKI HYDRAULICZNE PODNOŚNIKA POWIETRZNEGO

ABSTRAKT

Podnośniki powietrzne są najprostszymi urządzeniami wykorzystywanymi do podnoszenia i transportu cieczy w systemach wodnych i kanalizacyjnych. Ze względu na przepływ dwufazowy są one przedmiotem wielu badań. Znajomość parametrów przepływu dwufazowego jest niezbędna do właściwego zaprojektowania podnośnika. W dostępnej literaturze można znaleźć wiele modeli opisujących przepływy mieszaniny ciecz–gaz. Jednym z bardziej popularnych jest model Zuber-Findlaya (tzw. poślizgowy).

Przedmiotem badań była kolumna barbotażowa służąca do transportu mieszaniny woda–powietrze o średnicach 50 i 75 mm. Na podstawie uzyskanych wyników sporządzono charakterystyki hydrauliczne: wydajności podnośnika w zależności od głębokości zanurzenia oraz od ilości doprowadzanego powietrza. Do opisu matematycznego zastosowano model w postaci wielomianu drugiego stopnia i przeprowadzono ocenę współczynnika determinacji. Określono sprawność podnośnika powietrznego oraz na podstawie modelu poślizgowego określono parametry mieszaniny dwufazowej podczas jego pracy.

Stwierdzono, że wydajność podnośnika rośnie wraz ze wzrostem głębokości zanurzenia oraz ilości doprowadzanego powietrza; urządzenie osiąga maksymalną sprawność w określonym zakresie głębokości zanurzenia. W podnośniku powietrznym o małej średnicy (50 mm) dominuje rzutowa struktura przepływu.

Słowa kluczowe: podnośnik powietrzny, przepływ dwufazowy, sprawność podnośnika powietrznego